Title
Simplified algorithms for calculating double-couple rotation

Journal
Geophysical Journal International, 171(1)

Author
Kagan, Yan Y.

Publication Date
2007-10-01

DOI
10.1111/j.1365-246X.2007.03538.x

Peer reviewed

Geophys. J. Int. (2007) **000**, 1–7

Simplified algorithms for calculating double-couple rotation

Yan Y. Kagan

Department of Earth and Space Sciences, University of California, Los Angeles, California 90095-1567, USA;
Phone: 310-206-5611; Fax: 310-825-2779; E-mail: ykagan@ucla.edu, kagan@moho.ess.ucla.edu

Accepted 2007 June 27. Received 2007 June 27; in original form 2007 May 5

SUMMARY

We derive new, simplified formulae for evaluating the 3-D angle of earthquake double couple (DC) rotation. The complexity of the derived equations depends on both accuracy requirements for angle evaluation and the completeness of desired solutions. The solutions are simpler than my previously proposed algorithm based on the quaternion representation designed in 1991. We discuss advantages and disadvantages of both approaches. These new expressions can be written in a few lines of computer code and used to compare both DC solutions obtained by different methods and variations of earthquake focal mechanisms in space and time.

Key words: Earthquake-source mechanism, Fault-plane solutions, Seismic moment, Seismotectonics, Statistical methods, Inverse problem

doi: 10.1111/j.1365-246X.2007.03538.x
PostScript file created: 30 August 2007; time 961 minutes

1 INTRODUCTION

A large number of traditional fault plane and moment tensor solutions is presently available. Thus, for individual events we can study varying focal mechanisms to see whether they yield any information regarding the spatial orientations of the earthquakes and microearthquakes that comprise a fault system (Kagan 2006). Additionally a simple method is needed to compare focal mechanism solutions obtained by different methods. For accessible discussion of earthquake focal mechanisms see Jost & Herrmann (1989) and Pujol & Herrmann (1990). Methods for determining focal mechanism are discussed by Ekström *et al.* (2005, and references therein) and by Snoke (2003).

In this paper we consider three-dimensional (3-D) rotations by which one double-couple (DC) earthquake source can be turned into another arbitrary DC. Presently different orientations of earthquake focal mechanisms are studied by separately displaying 2 or 3 DC axes on an equal-area plot (see, for example, Bressan *et al.* 2003). Kagan (1991) published an algorithm to determine the 3-D rotation parameters of a DC earthquake source. That method was based on transforming a focal mechanism solution to a normalized quaternion, and the problem of the 3-D rotation was solved by applying quaternion algebra (Altmann 1986). Kuipers (2002) and Hanson (2005) present a more accessible mathematical treatment of 3-D rotations with many explicit formulae.

Due to the symmetry of DC sources, there are four possible rotations with the angle less or equal to 180° between two different mechanisms. This symmetry also means that the standard methods for determining 3-D rotation (see the citations above) need modifications to accommodate it. Thus, four different rotation angles and four rotation pole positions (the intersection of the rotation axis with a reference sphere) need to be found. Two spherical coordinates on a reference sphere can be used to describe each pole.

The quaternion method (Kagan 1991) has been used to evaluate these rotations in many investigations of earthquake focal mechanisms (see, for example, Frohlich & Davis 1999; Kagan & Jackson 2000; Kagan 2003; Bird & Kagan 2004; Okal 2005; Pondrelli *et al.* 2006; Matsumoto *et al.* 2006). Among these applications are finding a difference in focal mechanism solutions obtained through diverse methods; analysis of seismicity patterns; investigating connections between tectonic stress fields and earthquake source mechanisms, and so on. Kagan (1991, Section 4) mentioned other possible uses of the algorithms for calculating DC rotation.

For most of these studies, only the minimum rotation angle between two focal mechanism solutions was considered. This angle can be obtained by a simple formula. The relatively complex original quaternion programme (Kagan 1991) was created in FORTRAN, a computer language not widely used now. (However, P. Bird recently reworked the programme in FORTRAN90, it is available from his Web site ftp://element.ess.ucla.edu/2003107-esupp/Quaternion.f90). In contrast, the equations in this paper can be easily programmed in any software by a few lines of code. Moreover, since the knowledge of quaternions is not common among geophysicists, we largely avoid their use here.

We first describe how to calculate the minimum 3-D rotation angle between two focal mechanism solutions, starting with the simplest methods. Then we obtain expressions for all four angles and rotation pole positions. Initially, we describe algorithms that can be used with the original focal mechanisms presented in earthquake catalogues. Thereafter, we consider those transformations necessary to obtain a more complete and accurate description of the 3-D rotations. These rotation variables may be used in more extensive investigations of earthquake occurrence geometry and mechanics.

2 DOUBLE COUPLE REPRESENTATION

A seismic moment tensor is a symmetric 3×3 matrix

$$m = \begin{vmatrix} m_{11} & m_{12} & m_{13} \\ m_{21} & m_{22} & m_{32} \\ m_{31} & m_{32} & m_{33} \end{vmatrix}, \quad (1)$$

and it has six degrees of freedom. The moment tensor is assumed to be traceless or deviatoric (Aki & Richards 2002), i.e., its first invariant is equal to zero, $I_1(m) = 0$; hence the tensor number of degrees of freedom is five.

Moreover, there is significant statistical evidence (Frohlich & Davis 1999; Kagan 2003; Frohlich 2006, pp. 228-235) that for most tectonic earthquakes, the moment tensor can be approximated by a DC source. This means that the third invariant of the moment tensor is also zero, $I_3(m) = 0$. Thus, the parameter number is four. If we consider a normalized solution, this reduces the total number of degrees of freedom to three.

The normalized eigenvectors of matrix (1) are vectors

$$\begin{aligned} \mathbf{t} &= [1, 0, 0]; \\ \mathbf{p} &= [0, 1, 0]; \\ \mathbf{b} &= [0, 0, 1]. \end{aligned} \quad (2)$$

Three orthogonal axes $\mathbf{t}$, $\mathbf{p}$, and $\mathbf{b}$ describe the radiation of P-waves from a point DC source (Frohlich 1996; Aki & Richards 2002). Since the tensor is symmetric, the direction of vectors can be selected arbitrarily; traditionally the axes are directed downwards. Each axis is parameterized by two angles: plunge α and azimuth β. The normalized DC source is defined by three degrees of freedom, therefore three of these angles can be calculated if the other three are known.

The orientation matrix of a focal mechanism solution is the direction cosine matrix (DCM)

$$\mathbf{D} = \begin{vmatrix} t_1 & p_1 & b_1 \\ t_2 & p_2 & b_2 \\ t_3 & p_3 & b_3 \end{vmatrix}, \quad (3)$$

where each vector coordinate is calculated as, for example,

$$\begin{aligned} t_1 &= \cos(\alpha_t)\cos(\beta_t); \\ t_2 &= \cos(\alpha_t)\sin(\beta_t); \\ t_3 &= \sin(\alpha_t), \end{aligned} \quad (4)$$

where α_t and β_t are the plunge and the azimuth of the $\mathbf{t}$-axis.

All columns and rows of the orthogonal matrix (3) are normalized orthogonal vectors; hence, for example

$$t_3^2 + p_3^2 + b_3^2 = 1, \quad (5)$$

or

$$\sin^2\alpha_t + \sin^2\alpha_p + \sin^2\alpha_b \;=\; 1\,, \tag{6}$$

where α_t is **t**-axis plunge angle, etc. (Frohlich 1992).

The determinant of the matrix $\mathbf{D}$ (Eq. 3) is

$$\begin{aligned}\mathrm{Det}\,(\mathbf{D}) \;=\; I_3 \;=\;\; & t_1p_2b_3 + t_2p_3b_1 + t_3p_1b_2 - \\ & t_1p_3b_2 - t_2p_1b_3 - t_3p_2b_1\,,\end{aligned} \tag{7}$$

where I_3 is the third invariant of the matrix and is equivalent to the determinant. For the *proper* rotation matrix, the determinant is 1.0. If it is equal -1.0, the transformation is a rotation plus a reflection or an improper rotation.

As mentioned above, to make the focal mechanism representation unique, the eigenvectors are pointed down. However, the handedness of the coordinate system formed by the vectors can change as the result of such an assignment. In most of our considerations, we use the right-handed coordinate system (*cf.*, Kuipers 2002, pp. 47-48, 143; Altmann 1986, pp. 29, 52), centered on each earthquake centroid. We use the **t**-, **p**-, and **b**-axes of the earthquake focal mechanism as coordinate axes.

In Fig. 1 we display an example of the right-handed coordinate system for a DC source. The system can be arbitrarily rotated, and the handedness of the system is preserved. The left-handed system can be obtained in this picture if one inverts the direction of any individual axis.

If no vector has a 90° plunge, we can look at their surface projection; the clockwise **tpb** arrangement corresponds to the right-hand system and the **tbp** corresponds to the left-hand. Otherwise, the handedness can be found by calculating the matrix determinant (7); if it is equal to -1, the system is left-handed. In principle, rigid rotation can be defined for the left-handed systems. However, in that case the handedness should be kept uniform over the whole focal mechanism set.

The system shown in Fig. 1 corresponds to the identity matrix

$$\mathbf{I} \;=\; \begin{vmatrix} 1 & 0 & 0 \\ 0 & 1 & 0 \\ 0 & 0 & 1 \end{vmatrix}\,, \tag{8}$$

where all the axes have coordinates as in (2).

To insure the 'right-handedness' of the system, we preserve the downward direction of the **t**- and **p**-axes, as given in the catalogues of the fault-plane solutions. However, the direction of the **b**-axis is chosen according to the right-hand rule. This can be accomplished either by inspecting the configuration of the axes, or by calculating the **b**-axis coordinates as a vector product of the **t**- and **p**-axes. We will call this system the **tpb**-system of coordinates.

3 ROTATION REPRESENTATION

The orientation DCM matrix (3) can be considered a rotation matrix which transforms the identity matrix (8) into one corresponding to a particular DC solution. For any vector $\mathbf{v}_0$, the rotated vector $\mathbf{v}$ is

$$\mathbf{v} \;=\; \mathbf{D}\,\mathbf{v}_0\,, \tag{9}$$

or

$$\mathbf{v}_0 \;=\; \mathbf{D}^T\,\mathbf{v}\,, \tag{10}$$

where $\mathbf{D}^T$ is a transposed matrix.

Thus, for two vectors or two rotated systems of coordinates like (3) we can obtain

$$\mathbf{v}' \;=\; \mathbf{D}_1\,\mathbf{D}_2^T\,\mathbf{v}'' \;=\; \mathbf{R}\,\mathbf{v}''\,, \tag{11}$$

where $\mathbf{R}$ is an orthonormal rotation matrix: a matrix product of two orientation (DCM) matrices. The elements of $\mathbf{R}$ are calculated as

$$\begin{aligned} R_{11} &= t_1'\,t_1'' + p_1'\,p_1'' + b_1'\,b_1''\,; \\ R_{12} &= t_1'\,t_2'' + p_1'\,p_2'' + b_1'\,b_2''\,; \\ R_{21} &= t_2'\,t_1'' + p_2'\,p_1'' + b_2'\,b_1''\,, \end{aligned} \tag{12}$$

and so on.

For the rotation matrix $\mathbf{R}$, the rotation angle Φ is (Kuipers 2002, pp. 57, 163)

$$\begin{aligned}\Phi &= \arccos\{[\,\mathrm{Tr}\,(\mathbf{R}) - 1]\,/2\} \\ &= \arccos\left[\frac{R_{11} + R_{22} + R_{33} - 1}{2}\right]\,,\end{aligned} \tag{13}$$

where $\mathrm{Tr}\,(\mathbf{R})$ is the trace of the matrix $\mathbf{R}$ and $180^\circ \;\geq\; \Phi \;\geq\; 0^\circ$. Using (12) we obtain

$$\begin{aligned} R_{11} + R_{22} + R_{33} \;=\;\; & t_1'\,t_1'' + p_1'\,p_1'' + b_1'\,b_1'' + \\ & t_2'\,t_2'' + p_2'\,p_2'' + b_2'\,b_2'' + \\ & t_3'\,t_3'' + p_3'\,p_3'' + b_3'\,b_3''\,, \end{aligned} \tag{14}$$

or

$$R_{11} + R_{22} + R_{33} \;=\; \mathbf{t}'\cdot\mathbf{t}'' \;+\; \mathbf{p}'\cdot\mathbf{p}'' \;+\; \mathbf{b}'\cdot\mathbf{b}''\,, \tag{15}$$

where $\mathbf{t}'\cdot\mathbf{t}''$ is a dot product of two vectors

$$\mathbf{t}'\cdot\mathbf{t}'' \;=\; t_1'\,t_1'' \;+\; t_2'\,t_2'' \;+\; t_3'\,t_3''\,. \tag{16}$$

Coordinates of the rotation axis **e**, i.e., axis which is invariant during the rotation, are computed as (Kuipers 2002, p. 66)

$$\begin{aligned} e_1 &= (R_{23} - R_{32})/\sin(\Phi)\,; \\ e_2 &= (R_{13} - R_{31})/\sin(\Phi)\,; \\ e_3 &= (R_{12} - R_{21})/\sin(\Phi)\,. \end{aligned} \tag{17}$$

Thus, for example, (see Eq. 12)

$$\begin{aligned} e_3 \;=\;\; & \left[(t_1'\,t_2'' - t_2'\,t_1'') + (p_1'\,p_2'' - p_2'\,p_1'')\right. \\ & \left. + (b_1'\,b_2'' - b_2'\,b_1'')\,\right]/\sin(\Phi)\,. \end{aligned} \tag{18}$$

4 DOUBLE COUPLE ROTATION

4.1 Minimum rotation angle evaluation

4.1.1 Rotation angle $\Phi \;\leq\; 90^\circ$

As a rule, the handedness of the coordinate system is invariant if we change the direction of any two axes. In 3-D there are four possibilities: the original coordinate configuration and three pair inversions. In the eigenvector matrix (3) all axes can be inverted pairwise; as we will see later (Section 4.2), this explains why a DC source can be rotated by four different rotations into another source ($180^\circ \;\geq\; \Phi \;\geq\; 0^\circ$).

Practical applications often use the minimum angle of the four rotation angles. Thereafter, unless specified otherwise, we use the notation

$$\Phi \;=\; \Phi_{\rm min}\,. \qquad (19)$$

The minimum value for Φ is zero, when both solutions are identical. The maximum Φ-value depends on the direction of a rotation axis.

Fig. 2 displays the *maximum* values of the *minimum* rotation angle

$$\Phi_{\rm max} \;=\; \max(\,\Phi\,)\,, \qquad (20)$$

in one octant in a coordinate system formed by eigenvectors of the moment matrix (1). The angles are shown in the system coordinates formed by the axes of the first DC source (see also below Eqs. 34 and 35). Since the angle pattern has a C_3 symmetry (Altmann 1986), the axis order is irrelevant, so instead of the **tpb** axes, we indicate **1-2-3** axes in the plot. Therefore, the $\Phi_{\rm max}$-value for a DC source is at least 90° and cannot exceed 120°

$$120^\circ \;\geq\; \Phi_{\rm max} \;\geq\; 90^\circ\,, \qquad (21)$$

(Kagan 1991; Frohlich & Davis 1999).

As Eqs. 13-16 suggest, to determine angle Φ we need to know the dot products of the focal mechanism axes. Each of the dot products $\mathbf{t}'\cdot\mathbf{t}''$, $\mathbf{p}'\cdot\mathbf{p}''$, and $\mathbf{b}'\cdot\mathbf{b}''$ (see Eq. 16), are cosines of angles γ_i between two orientations of the coordinate axes, e.g.,

$$\gamma_t \;=\; \arccos(\,\mathbf{t}'\cdot\mathbf{t}''\,)\,, \qquad (22)$$

etc.

The angles γ_i, arbitrarily permuted, should satisfy the triangle rule

$$\gamma_1 \;\leq\; \gamma_2 + \gamma_3\,. \qquad (23)$$

For relatively small angles,

$$\cos\Phi \;\approx\; 1 - \Phi^2/2\,, \qquad (24)$$

and (see Eqs. 13-15)

$$\Phi_{\rm sm} \;\approx\; \sqrt{\frac{\gamma_t^2+\gamma_p^2+\gamma_b^2}{2}}\,. \qquad (25)$$

Angle Φ satisfies inequalities

$$\gamma_{\rm max} \;\leq\; \Phi \;\leq \gamma_{\rm max}\sqrt{3/2}\,, \qquad (26)$$

where $\gamma_{\rm max}$ is the maximum of the coordinate axis angles.

If the 3-D rotation is around any of the eigenvector axes, one of the γ-angles is zero, and the other two are equal. In this case (25) is exact. The maximum error ε in using (25) is reached when all γ-angles are equal, and the rotation axis is inclined to all the axes at the angle $\arccos(\,1/\sqrt{3}\,) \approx 54.74^\circ$ (Kagan 2005)

$$\varepsilon \;\leq\; \arccos[\,(3\cos\gamma - 1)/2\,] \;-\; \gamma\sqrt{3/2}\,. \qquad (27)$$

See Eqs. 13, 25, and Eq. 29 below.

Since angles γ_i are between the axes, they should not exceed 90°. Hence the dot products (16) may be made greater or equal to zero. Thus, the simplest formula for the minimum rotation angle Φ calculation is an adaptation of (13)

$$\Phi \;=\; \arccos\left[\frac{1}{2}\left(\,|\,\mathbf{t}'\cdot\mathbf{t}''\,|\,+|\,\mathbf{p}'\cdot\mathbf{p}''\,|\,+|\,\mathbf{b}'\cdot\mathbf{b}''\,|\,-1\right)\right]. \qquad (28)$$

This formula yields the correct value of the rotation angle for $\Phi \;<\; 90^\circ$. The coordinate system handedness of both solutions can be arbitrary. However, if $\Phi \;>\; 90^\circ$ (28), can produce an angle value which exceeds 90°, but is incorrect by being too small. It occurs because the rigid rotation $\Phi \;>\; 90^\circ$ may result in one of the axis dot products (16) being negative. Thus, if Eq. 28 is used, the direction of the axis has been reversed, producing the system configuration of the opposite handedness. In this case the rotation angle is not properly defined.

In Fig. 3 we display the error curve (27) as well as the values of the rotation angle Φ for magnitude $M \geq 6.0$ shallow (depth 0-70 km) earthquakes in the CMT catalogue (Ekström *et al.* 2005). These angles are calculated by Eq. 28 and by the approximate formula (25). The difference is plotted against Φ. The small difference is not surprising, because (24) is accurate within 1% for angles up to 38°. The maximum error is less than 0.5° for $\Phi < 45^\circ$, and since the best accuracy of the Φ determination is above 10° (Kagan 2000; 2003), Eq. 25 can be used for most calculations.

4.1.2 Rotation angle $\Phi \;\geq\; 90^\circ$

In Table 1 we show the number of negative dot products that can be obtained for two arbitrary DC solutions. If the orientation of these solutions is opposite (shown in Table 1 by their determinants I_3 to be of different signs), we can change the vector's sign. This change reduces or increases the number of negative dot products by one. Two negative dot products can be inverted without changing the system's handedness.

Thus, if the rotation angle derived by using (28) exceeds 90°, we need to check the handedness of both solutions and the number of negative dot products to obtain the correct Φ value. If these numbers are the same as in the second or third column of Table 1, the Φ estimate is correct. If these numbers are like those in the last column of the Table, the angle is incorrect (see below Eq. 30 and the explanation). Thus, we must use a more general equation to obtain the minimum angle

$$\Phi_i \;=\; \arccos\left[\frac{1}{2}\left(\,\mathbf{t}'\cdot\mathbf{t}'' + \mathbf{p}'\cdot\mathbf{p}'' + \mathbf{b}'\cdot\mathbf{b}'' - 1\right)\right]. \qquad (29)$$

For $\Phi \;>\; 90^\circ$ to obtain the minimum rotation angle Φ in the above formula, the smallest absolute value dot product should be negative, and the other products should be positive. Since the direction of any vector pair can be altered without changing the handedness of the rotation matrix (Section 2), there are ordinarily four different angles $\Phi_i \;\leq\; 180^\circ$ for rotating one DC solution into another.

To understand why the solutions behaviour changes when $\Phi \;\geq\; 90^\circ$, note the expression of the rotation matrix diagonal terms (Kuipers 2002, Eq. 7.16) through the rotation angle and the rotation axis coordinates (17)

$$\begin{aligned}
\mathbf{t}'\cdot\mathbf{t}'' \;&=\; \cos\gamma_t \;=\; e_1^2 + (e_2^2+e_3^2)\cos\Phi\,;\\
\mathbf{p}'\cdot\mathbf{p}'' \;&=\; \cos\gamma_p \;=\; e_2^2 + (e_3^2+e_1^2)\cos\Phi\,;\\
\mathbf{b}'\cdot\mathbf{b}'' \;&=\; \cos\gamma_b \;=\; e_3^2 + (e_1^2+e_2^2)\cos\Phi\,. \qquad (30)
\end{aligned}$$

If $\Phi \;\leq\; 90^\circ$, $\cos\Phi \;\geq\; 0$, and thus all the axes dot products are positive, and $\gamma_i \;\leq\; 90^\circ$. However, if $\Phi \;>\; 90^\circ$, depending on the values of the rotation axis coordinates, some dot products may become negative. For $\Phi \;=\; 120^\circ$ all the dot products are zero, because the DC eigenvectors exchange their directions and the γ-angles between all axes are 90° (see Frohlich & Davis 1999, Fig. 3).

Using (30), we calculate the angle $\Phi_{\mathbf{neg}}$. For rotation angle

$$\Phi_{\mathbf{max}} \geq \Phi \geq \Phi_{\mathbf{neg}}\,, \tag{31}$$

(see Eq. 20) at least one of the dot products becomes negative. In Fig. 4 we display the difference of two angles $\Phi_{\mathbf{max}} - \Phi_{\mathbf{neg}}$ (the distribution of the $\Phi_{\mathbf{max}}$ angle is shown in Fig. 2). The maximum difference (more than 18°) is for a rotation vector between any two axes. For a rotation pole in this part of the reference sphere, if $\Phi > 90°$, all or almost all appropriate dot products are the same as in the last column of Table 1.

Fig. 5 shows the distribution of solutions with negative dot products in the CMT catalogue (Ekström *et al.* 2005). The rotation poles are concentrated according to the isolines in Fig. 4. In Fig. 6 we display the position of the rotation poles when the rotation angle is restricted to $\Phi \geq 105°$. Here the pattern is influenced by both angle distributions, shown in Figs. 2 and 4.

4.2 Rotation vector determination

To obtain the rotation vector coordinates (17), we proceed similarly to calculation Φ_i by Eq. 29. For example, in Eq. 18 we change the sign of any pair of vectors. This leads to the sign change of the dot products in Eq. 29. Such a change would reverse the sign for two arbitrary terms in ordinary brackets of (18). Thus, we obtain simultaneously a set of four angles Φ_i and their rotation axes $\mathbf{e}_{(i)}$.

The spherical coordinates (colatitude θ and azimuth ψ) of the rotation pole on a reference sphere can also be computed as

$$\theta = \arccos(e_3)\,. \tag{32}$$

and

$$\psi = \arctan(e_2/e_1)\,, \tag{33}$$

$\theta = 0°$ correspond to the vector pointing down. Signs of e_1 and e_2 must be noted to properly calculate the azimuth: $360° > \psi \geq 0°$.

The above calculations provide the pole position at the local geographic system. If we want to investigate the DC rotation as seen, for instance, from the first DC source, we need to rotate the reference sphere accordingly

$$\mathbf{e}' = \mathbf{D}_1^T\,\mathbf{e}\,. \tag{34}$$

Rotation angles Φ_i are not influenced by this transformation.

We illustrate the computations in Tables 2 and 3. Table 2 shows four pairs of earthquakes from the CMT catalogue (Ekström *et al.* 2005). We display their focal mechanisms in Fig. 7. In the last column of Table 2 we show the determinant of the DCM matrix (3) for the DC focal mechanism of each event.

Table 3 shows axis dot products, the rotation angles, and coordinates of rotation poles for all the earthquake pairs from Table 2. In the first line for each event pair, the minimum angle Φ is evaluated using a simple formula (28) or (29).

For the first earthquake pair in Table 3, inspecting the numbers of negative dot products and comparing them to Table 1 values, we see that Eq. 28 would yield an incorrect answer, so (29) should be used to calculate Φ (row 1). In the subsequent rows (2-5) we show the parameters of four rotations for each pair determined as discussed above. Before carrying out this evaluation, the handedness of both solutions was adjusted to be consistent. For other earthquake couples, Eq. 28 is sufficient to calculate Φ (rows 6, 11, and 16).

As Eq. 17 shows, the rotation vector $\mathbf{e}$ coordinates determination is impossible when $\sin\Phi = 0$. This corresponds either to $\Phi = 0°$ or $\Phi = 180°$. The latter case is the binary rotation (Altmann 1986). The algorithm failure to determine the rotation axis coordinates is connected with unavoidable singularities in working with the rotation matrices and the Euler angles (Kuipers 2002, pp. 74, 152). For these rotations, off-diagonal terms in the rotation matrix $\mathbf{R}$ are either zero or have the same value, so the $\mathbf{e}$ coordinate values in (17) are zero.

Only the quaternion application enables us to consistently avoid this difficulty. The parameters determined by using the quaternion technique (Kagan 1991) in Table 3 are usually the same as those obtained from rotation matrix analysis. However, as explained above, the coordinates of the rotation axis for $\Phi = 180°$ are not defined in the latter case. In Table 3 we illustrate this in rows 9 and 10, where the rotation axis coordinates are obtained from the quaternion representation.

As we indicate in (34), if the rotation pole coordinates are preferred in the system connected with the first DC, we should recalculate the rotation vector $\mathbf{e}$. As an example, we perform such a computation for the first solution pair in Table 3 (row 2)

$$\begin{aligned}
\mathbf{D}_1^T &= \begin{matrix} 0.1187 & 0.7439 & 0.6577 \\ 0.2813 & -0.6604 & 0.6962 \\ 0.9522 & 0.1024 & -0.2877\,; \end{matrix} \\
\mathbf{e}_1 &= 0.9026, \quad -0.3227, \quad 0.2850\,; \\
\mathbf{e}_1' &= 0.0545, \quad 0.6655, \quad 0.7444\,.
\end{aligned} \tag{35}$$

The new colatitude θ' and azimuth ψ' of the rotation pole are:

$$\theta' = 41.9°,\ \phi' = 85.3°,\ \text{and}\ \Phi = 99.1°\,. \tag{36}$$

Using Eqs. 26-29 by Kagan (2005) we can convert the rotation vector coordinates into equal-area octant projection $X = 0.451$ and $Y = 0.327$. This point is shown in Fig. 5. As another example, the rotation axis from row 7 of Table 3 would coincide with the **b**-axis (its coordinates are $X = 0.0$ and $Y = 0.919$, not shown in Fig. 5).

In general, Eqs. 13-26 are valid if the γ_i angles are measured between two different DC solutions, i.e., we can calculate a 3-D rotation angle Φ from these measurements. However, although all the γ_i have three degrees of freedom (the same number required to characterize the 3-D rotation), the latter angles do not fully specify the 3-D rotation. It is possible to obtain the rotation angle (Φ) from the angle differences (γ_i) for three axes, but we cannot obtain a unique set of the rotation axis components.

Since the cosines of the angles are expressed through squares of the quaternion components, $2^4 = 16$ different quaternions (and eight rotations, since quaternions of opposite signs characterize the same rotation) correspond to a

set of coordinate axis components (Kagan 1991; 2005). Similar conclusions can be derived from Eq. 25. The rotation poles for a set of three dot products are situated in all eight octants of the reference sphere. Hence, there are eight rotations having the same angle Φ and the same dot products of coordinate axes. These eight should not be confused with four rotations transforming one DC source into another. The number of these rotations is due to the symmetry of the DC.

4.3 Computational considerations

The plunge (α) and the azimuth (β) angles (as in Eq. 4) are usually rounded off to integer values in earthquake catalogues. This may cause two problems: (a) the accuracy of angles (γ in Eq. 22 or Φ_i in Eq. 29) determination cannot exceed 1° and (b) axes are not exactly orthogonal. The second condition may cause difficulties in further analysis of the rotation. Correction methods for orthogonality and low precision are not unique. Therefore, different techniques may lead to differences in the final results (sometimes as large as 1° to 2°).

Kagan (1991) avoided these difficulties by orthogonalizing axes and calculating the **b**-axis to form the right-hand coordinate system (see Section 2). Another solution would be to calculate eigenvectors of the matrix (1) with sufficient precision and carry out the computations with those values.

Finally, for user convenience we would present equations to obtain eigenvectors from geologic/tectonic representation of earthquake focal mechanisms (Kagan 2005). Such representation is common in catalogues based on first-motion focal mechanism determination. The standard parameterization of a fault rupture plane involves defining its strike (azimuth) ϕ, dip δ, and rake λ (Aki & Richards 2002). The plane orthogonal to the fault plane and slip vector is an auxiliary nodal plane.

Coordinates of the eigenvectors can be obtained from both sets of ϕ, δ, and λ angles

$$\begin{aligned}
t_1 &= (-\sin\phi\sin\delta + \cos\phi\cos\lambda + \sin\phi\cos\delta\sin\lambda)/\sqrt{2}\,;\\
t_2 &= (\cos\phi\sin\delta + \sin\phi\cos\lambda - \cos\phi\cos\delta\sin\lambda)/\sqrt{2}\,;\\
t_3 &= (-\cos\delta - \sin\delta\sin\lambda)/\sqrt{2}\,;\\
p_1 &= (-\sin\phi\sin\delta - \cos\phi\cos\lambda - \sin\phi\cos\delta\sin\lambda)/\sqrt{2}\,;\\
p_2 &= (\cos\phi\sin\delta - \sin\phi\cos\lambda + \cos\phi\cos\delta\sin\lambda)/\sqrt{2}\,;\\
p_3 &= (-\cos\delta + \sin\delta\sin\lambda)/\sqrt{2}\,;\\
b_1 &= \cos\phi\sin\lambda - \sin\phi\cos\delta\cos\lambda\,;\\
b_2 &= \sin\phi\sin\lambda + \cos\phi\cos\delta\cos\lambda\,;\\
b_3 &= \sin\delta\cos\lambda\,. \qquad (37)
\end{aligned}$$

The vectors' direction can be inverted downwards if needed.

5 DISCUSSION

Double-couple earthquake mechanisms can be described fully by specifying three mutually perpendicular axes. When comparing two DCs, it is often useful to know what rotation angles about what axis would transform one solution into the other. Kagan (1991) showed how to do this with quaternions. In this paper we explain how 'ordinary' matrices and vectors can be used to obtain 3-D rotation parameters.

The orthogonal matrix **D** or any other orthonormal matrices discussed above can be converted to the quaternion representation (Kagan 1991; Hanson 2005, pp. 148-150). Although both approaches can be viewed as equivalent, Hanson (2005, Ch. 16) argues that for many applications vector operations are more efficient computationally. However, the quaternion technique has many advantages.

Representing a 3-D rotation as a quaternion (4 numbers) is more compact than representing it as an orthogonal matrix (9 values). Furthermore, for a given axis and angle, one can easily construct the corresponding quaternion, and conversely, for a given quaternion one can easily read off the axis and the angle. This is harder to do with matrices or Euler angles (see Altmann 1986; Kuipers 2002; Hanson 2005; a more compact and accessible description can be obtained from the Wikipedia by 'Googling', for instance, *Rotation representation*, etc.).

When composing several rotations on a computer, rounding errors necessarily accumulate. A quaternion that is slightly off still represents a rotation after being normalized. However, a matrix that is slightly off need not be orthogonal and is therefore harder to convert back to its proper form.

The quaternion treatment, generally, is superior in its elegance and simplicity, especially for handling a sequence of rotations (Kuipers 2002; Hanson 2005). For example, Kagan (1982) used the quaternion formalism to simulate propagation of an earthquake fault with stochastic 3-D rotations of micro-dislocations. Moreover, as we have seen above, other representations of 3-D rotations experience singularities. In the quaternion representation of 3-D rotations, that problem is avoided (Kuipers 2002, pp. 74, 152).

An additional obstacle to determine the rotation parameters of earthquake sources is the symmetry of the DC focal mechanism. As we have seen in Sections 4.1 and 4.2, when using orthonormal matrices and eigenvector dot products, significant complications must be overcome if the rotation angle exceeds 90°. Again, quaternion algebra allows for taking the DC symmetry into account (Kagan 1991) and processing all the input information automatically. Therefore, the advantage of simplicity for the orthonormal matrices method may decrease or even disappear, if we try to calculate all the DC rotation parameters.

6 CONCLUSIONS

Below we summarise the proposed algorithms for evaluating the rotation between two DC focal mechanism solutions. We start with the simpler methods:

- 1. In the beginning, the equality of two DC sources should be checked. This is needed because of angle values rounding off (see Section 4.3). For example, in the 1977-2004 CMT catalogue, 35 pairs of shallow earthquakes separated by less than 100 km have the same mechanism. If the mechanisms are equal, no further action is needed and more sophisticated algorithms may fail.
- 2. If only the minimum rotation angle Φ is needed and is relatively small, Eq. 25 is sufficient.
- 3. Again, if only the minimum rotation angle Φ is needed, and $\Phi < 90°$, Eq. 28 is sufficient.
- 4. If $\Phi \geq 90°$, the handedness of the solutions and the number of negative dot products should be checked. Then

use Eq. 29 with the instructions below it.

• 5. If we need all the four angles Φ_i, the handedness of both solutions should be corrected to be the same. We change the sign of two dot products in four combinations (as shown in Tables 2 and 3), and Eq. 29 is used again.

• 6. The position of the rotation vectors or the rotation poles on a reference sphere can be obtained by calculating the rotation matrix (Section 4.2). If needed, the pole position can be transformed for display in the system coordinates associated with an earthquake focal mechanism (34–36).

• 7. Finally, applying the quaternion technique (Kagan 1991) yields the necessary parameters for the four rotations, if one or two of the rotations are binary (Section 4.2). In addition, as a rule, rotation sequences of DC sources are significantly easier to construct by using the quaternion representation (Kuipers 2002; Hanson 2005).

ACKNOWLEDGMENTS

I appreciate partial support from the National Science Foundation through grant EAR 04-09890, as well as from the Southern California Earthquake Center (SCEC). SCEC is funded by NSF Cooperative Agreement EAR-0106924 and USGS Cooperative Agreement 02HQAG0008. Comments by C. Frohlich, by an anonymous reviewer and by the Associate Editor J. Trampert have been helpful in revision of the manuscript. Kathleen Jackson edited the final version. Publication 1092, SCEC.

References

Aki, K. & Richards, P., 2002. *Quantitative Seismology*, 2nd ed., Sausalito, Calif., University Science Books, 700 pp.

Altmann, S. L., 1986. *Rotations, Quaternions and Double Groups*, Clarendon Press, Oxford, pp. 317.

Bird, P., & Y. Y. Kagan, 2004. Plate-tectonic analysis of shallow seismicity: apparent boundary width, beta, corner magnitude, coupled lithosphere thickness, and coupling in seven tectonic settings, *Bull. Seismol. Soc. Amer.*, **94**(6), 2380-2399 (plus electronic supplement).

Bressan, G., Bragato, P.L., & Venturini, C., 2003. Stress and strain tensors based on focal mechanisms in the seismotectonic framework of the Friuli-Venezia Giulia region (Northeastern Italy), *Bull. Seismol. Soc. Amer.*, **93**(3), 1280-1297.

Ekström, G., A. M. Dziewonski, N. N. Maternovskaya & M. Nettles, 2005. Global seismicity of 2003: Centroid-moment-tensor solutions for 1087 earthquakes, *Phys. Earth Planet. Inter.*, **148**(2-4), 327-351.

Frohlich, C., 1992. Triangle diagrams: ternary graphs to display similarity and diversity of earthquake focal mechanisms, *Phys. Earth Planet. Inter.*, **75**, 193-198.

Frohlich, C., 1996. Cliff's nodes concerning plotting nodal lines for P, S_h, and S_v, *Seismol. Res. Lett.*, **67**(1), 16-24.

Frohlich, C., 2006. *Deep Earthquakes*, New York, Cambridge University Press, 573 pp.

Frohlich, C., & S. D. Davis, 1999. How well constrained are well-constrained T, B, and P axes in moment tensor catalogs?, *J. Geophys. Res.*, **104**, 4901-4910.

Hanson, A. J., 2005. *Visualizing Quaternions*, San Francisco, Calif., Elsevier, pp. 498.

Jost, M. L., & R. B. Herrmann, 1989. A student's guide to and review of moment tensors, *Seismol. Res. Lett.*, **60**(2), 37-57.

Kagan, Y. Y., 1982. Stochastic model of earthquake fault geometry, *Geophys. J. Roy. astr. Soc.*, **71**(3), 659-691.

Kagan, Y. Y., 1991. 3-D rotation of double-couple earthquake sources, *Geophys. J. Int.*, **106**(3), 709-716.

Kagan, Y. Y., 2000. Temporal correlations of earthquake focal mechanisms, *Geophys. J. Int.*, **143**(3), 881-897.

Kagan, Y. Y., 2003. Accuracy of modern global earthquake catalogs, *Phys. Earth Planet. Inter.*, **135**(2-3), 173-209.

Kagan, Y. Y., 2005. Double-couple earthquake focal mechanism: Random rotation and display, *Geophys. J. Int.*, **163**(3), 1065-1072.

Kagan, Y. Y., 2006. Why does theoretical physics fail to explain and predict earthquake occurrence?, in: *Lecture Notes in Physics*, **705**, pp. 303-359, P. Bhattacharyya & B. K. Chakrabarti (Eds.), Springer Verlag, Berlin–Heidelberg. http://scec.ess.ucla.edu/~ykagan/india_index.html

Kagan, Y. Y., & D. D. Jackson, 2000. Probabilistic forecasting of earthquakes, *Geophys. J. Int.*, **143**(2), 438-453.

Kuipers, J. B., 2002. *Quaternions and Rotation Sequences: A Primer with Applications to Orbits, Aerospace and Virtual Reality*, Princeton, Princeton Univ. Press., 400 pp.

Matsumoto, T., Y. Ito, H. Matsubayashi, & S. Sekiguchi, 2006. Spatial distribution of F-net moment tensors for the 2005 West Off Fukuoka Prefecture Earthquake determined by the extended method of the NIED F-net routine, *Earth Planet. Space*, **58**(1), 63-67.

Okal, E. A., 2005. A re-evaluation of the great Aleutian and Chilean earthquakes of 1906 August 17, *Geophys. J. Int.*, **161**(2), 268-282.

Pondrelli, S., S. Salimbeni, G. Ekström, A. Morelli, P. Gasperini & G. Vannucci, 2006. The Italian CMT dataset from 1977 to the present, *Phys. Earth Planet. Inter.*, **159**, 286-303.

Pujol, J., & R. B. Herrmann, 1990. A student's guide to point sources in homogeneous media, *Seismol. Res. Lett.*, **61**(3-4), 209-224.

Snoke, J. A., 2003. FOCMEC: FOcal MEChanism determinations, International Handbook of Earthquake and Engineering Seismology (W. H. K. Lee, H. Kanamori, P. C. Jennings, & C. Kisslinger, Eds.), Academic Press, San Diego, Chapter 85.12.
http://www.geol.vt.edu/outreach/vtso/focmec/

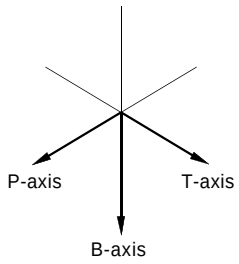

Fig. 1

Figure 1. Schematic diagram of earthquake focal mechanism. The right-hand coordinate system is used.

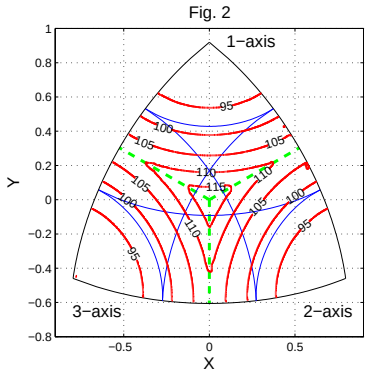

Figure 2. Isolines for maximum rotation angles ($\Phi_{\mathbf{max}}$, Eq. 20, shown in degrees) for various directions of a rotation axis for a DC source. The axis angles are shown at octant equal-area projection (Kagan 2005). Dashed lines are boundaries between different focal mechanisms. Plunge angles 30° and 60° for all axes are shown by thin solid lines. The smallest maximum rotation angle ($\Phi_{\mathbf{max}} = 90°$) is for rotation pole at any of eigenvectors, the largest angle (120°) is for the pole maximally remote from all the three vectors – in the middle of the diagram. The isogonal (Kagan 2005) maximum rotation angle (109.5°) corresponds to the pole position between any two eigenvectors – at remote ends of dashed lines.

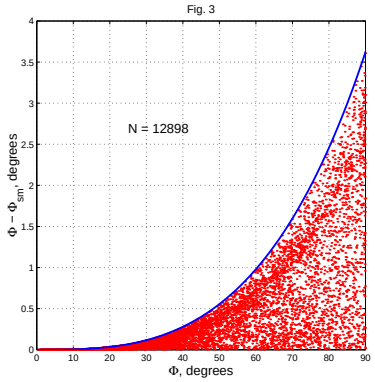

Figure 3. Dependence of error in Eq. 25 on the rotation angle Φ. Dots are errors for pairs of shallow earthquake solutions in the 1977-2004 CMT catalogue, separated by less than 100 km, N is the total number of pairs. Solid curve is the theoretical estimate (27) of the maximum error.

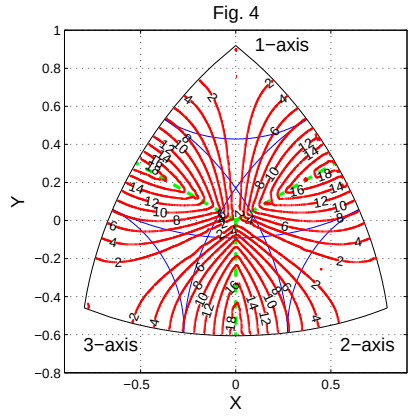

Figure 4. Isolines for rotation angles difference ($\Phi_{\mathbf{max}} - \Phi_{\mathbf{neg}}$, in degrees). Octant projection and auxiliary lines are the same as in Fig. 2. Angles $\Phi_{\mathbf{max}}$ are displayed in Fig. 2. The angles are shown in the system of coordinates formed by the axes of the first DC source (see Eqs. 34 and 35).

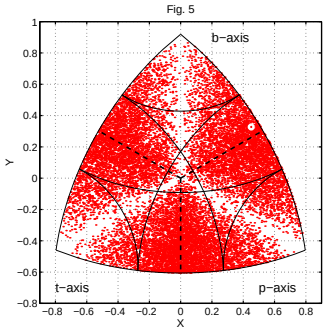

Figure 5. The distribution of rotation poles in solutions with negative dot products for $M \geq 5.0$ shallow (depth 0-70 km) earthquakes in the 1977-2004 CMT catalogue, separated by less than 100 km. The rotation angle is $\Phi \geq 90°$. The total number of pairs is 16,253. The position of the poles is shown in the system coordinates formed by the axes of the first DC source (34, 35). The rotation pole for row 2 in Table 3 is shown by a white circle (see Eq. 36 and below it). We show the positions of the **tpb**-axes in the plot.

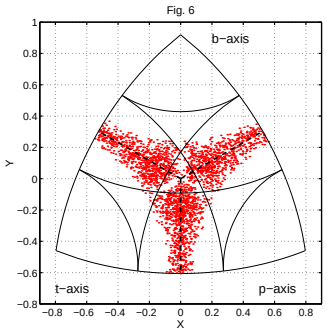

Figure 6. The distribution of rotation poles in solutions with negative dot products for $M \geq 5.0$ shallow earthquakes in the 1977-2004 CMT catalogue, separated by less than 100 km. The rotation angle is $\Phi \geq 105°$. The total number of pairs is 2,335. The position of the poles is shown in the system coordinates formed by the axes of the first DC source (see Eqs. 34 and 35).

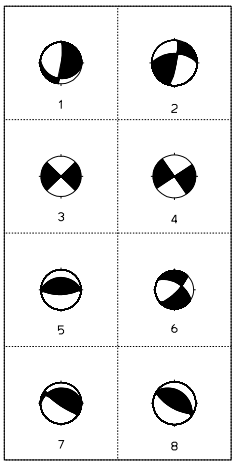

Figure 7. Focal mechanisms of earthquakes from Table 2. Lower hemisphere diagrams of focal spheres are shown, compressional quadrants (around the **t**-axis) are shaded. The numbers near diagrams correspond to the row numbers in Table 2.

Table 1. Number of negative dot products

Invariant relation	$\Phi < 90^\circ$	$\Phi > 90^\circ$	
		correct	incorr.
$I_3' = I_3''$	0, 2	0, 2	1, 3
$I_3' = -I_3''$	1, 3	1, 3	0, 2

I_3 is the third invariant (7) of the orientation DCM (3) matrix; it is determined for original catalogue data, therefore it can be positive for the right-handed configuration and *vice versa*. The second row corresponds to a different system orientation for both solutions.

Table 2. Earthquake pairs

#	Date	Time	t	p	b	I_3
			α, β	α, β	α, β	
1	1977/08/31	0:42:12.30	41,81	44,293	16,186	−1
2	1992/10/18	15:12:9.80	38,241	23,132	43,18	−1
3	1978/06/11	14:55:25.50	0,90	0,0	90,225	−1
4	1980/12/17	16:21:58.80	0,101	0,11	90,225	−1
5	1977/01/02	9:55:28.40	72,357	18,179	1,89	−1
6	1977/08/26	8:26:37.50	15,168	42,272	44,63	+1
7	1987/11/17	3:40:8.90	57,49	31,205	11,302	+1
8	1996/03/03	16:37:31.50	72,23	18,212	3,121	−1

I_3 is the third invariant (7) of an orientation DCM matrix; the positive invariant corresponds to the right-handed configuration and *vice versa*. The first number in the axis columns is the plunge α, the second number is the azimuth β, both in degrees.

Table 3. Rotation angles, Φ_i, and coordinates of rotation poles for several earthquake pairs from Table 2

#	E#	$\mathbf{t}' \cdot \mathbf{t}''$	$\mathbf{p}' \cdot \mathbf{p}''$	$\mathbf{b}' \cdot \mathbf{b}''$	Φ_i	θ	ψ
1	1,2	−0.155	−0.355	−0.484	**99.1**	–	–
2	1,2	−0.155	0.355	0.484	99.1	73.4	340.3
3	1,2	0.155	−0.355	0.484	111.0	98.2	215.2
4	1,2	0.155	0.355	−0.484	119.2	94.5	100.4
5	1,2	−0.155	−0.355	−0.484	175.2	165.4	347.0
6	3,4	0.982	0.982	1.0	**11.0**	–	–
7	3,4	0.982	0.982	1.0	11.0	0.0	0.0
8	3,4	−0.982	−0.982	1.0	169.0	180.0	0.0
9	3,4	0.982	−0.982	−1.0	180.0	*90.0*	*185.5*
10	3,4	−0.982	0.982	−1.0	180.0	*90.0*	*275.5*
11	5,6	−0.049	0.170	0.653	**93.7**	–	–
12	5,6	0.049	0.170	0.653	93.7	80.0	55.1
13	5,6	−0.049	−0.170	0.653	106.4	120.5	278.8
14	5,6	−0.049	0.170	−0.653	140.0	34.1	206.6
15	5,6	0.049	−0.170	−0.653	152.5	118.4	154.8
16	7,8	0.948	−0.969	−0.971	**19.2**	–	–
17	7,8	0.948	0.969	0.971	19.2	88.6	346.3
18	7,8	−0.948	−0.969	0.971	166.6	94.2	120.6
19	7,8	−0.948	0.969	−0.971	167.4	65.2	209.5
20	7,8	0.948	−0.969	−0.971	174.8	155.1	220.4

E# are the numbers of earthquake pairs from Table 2 (the first column). Bold-faced minimum rotation angles are evaluated by using (28) and (29). In these rows (1, 6, 11, and 16) the dot product signs are not adjusted, i.e., is calculated with the original catalogue data. Italic numbers in rows 9 and 10 are evaluated by using the quaternion representation.